



A promising Pd/polyaniline/foam nickel composite electrode for effectively electrocatalytic degradation of methyl orange in wastewater

Tingting Zhang^{a,b}, Jingli Zhang^{a,b,*}, Decheng Zou^{a,b}, Fang Cheng^{a,b}, Runxi Su^{a,b}

^aSchool of Environmental and Municipal Engineering, Tianjin Chengjian University, Tianjin 300384, China, Tel. +86 22 23085119; email: 15732029367@163.com (T. Zhang), Tel. +86 22 23085117; emails: jinglizhangczp@126.com (J. Zhang), 494008425@qq.com (D. Zou), chengfang10@sina.com (F. Cheng), surunxi@126.com (R. Su)

^bTianjin Key Laboratory of Aquatic Science and Technology, Tianjin Chengjian University, Tianjin 300384, China

Received 7 August 2019; Accepted 24 January 2020

ABSTRACT

This study was to enhance the electrochemical catalytic performance of the electrode. The foam nickel (Ni) electrode was modified by a two-step electrodeposition method to prepare a palladium/polyaniline/foam Ni electrode. The modified Ni electrode was characterized by scanning electron microscope, scanning cyclic voltammetry, and electrical impedance spectroscopy in comparison with the substrate electrode. The specific surface area and the electrical activity of the modified Ni electrode increased significantly and its charge transfer resistance decreased distinctly. The modified electrode was used for electrocatalytic degradation of methyl orange (MO) and the substrate Ni electrode was as control. The results showed the catalytic degradations of MO both fitted the first-order reaction model well at the voltage of 2 V and the rate constant k_{modified} (0.472 h^{-1}) was larger than $k_{\text{substrate}}$ (0.402 h^{-1}) for the two electrodes. The chemical oxygen demand removal rate (52%) of the modified electrode was higher than that (38%) of the substrate electrode. The ultraviolet-visible spectra showed that the modified electrode was more conducive to the degradation of MO and its intermediates. The degradation rates of azo dye and the decoloration rate decreased a little for five recycles under the voltage of 2 V, indicating that the modified electrode had good stability and could be reused.

Keywords: Modified foam nickel; Electrocatalytic degradation; Azo dye; Methyl orange

1. Introduction

Dyes, a widely existed contaminant in the wastewater due to the rapid development of the textiles, leather, and paper industries [1–8] are carcinogenic, mutagenic, and can lead to respiratory diseases [1,3,9,10]. Azo dyes account for 70% of all organic dyes produced in the world [11] and the azo bond in azo dyes, an electron-withdrawing group, contains a chromogenic group, making it difficult to biodegrade in natural water [7,12]. In general, methyl orange (MO), a typical azo dye, is regarded as the most difficult type to decompose [1,10], being more stable than other organic pollutants like Rhodamine B and methylene blue owing to the aromatic groups attached at each end of its azo bond [2].

Many methods are employed to treat azo dye wastewater, including advanced oxidation, biological, adsorption, electrochemical methods, and their combinations [2,13,14]. Advanced oxidation can oxidize various organic pollutants in water, but it requires a large number of strong oxidants, which increases the cost of such treatment [14,15]. The biodegradation has been considered a cost-effective and eco-friendly method of organic pollutant removal from wastewater [3,16], but it takes a long time for refractory organic matter. The adsorption process has simple operation and low equipment investment, but requires a large amount of adsorbent, and the regeneration of the adsorbent is difficult [9]. The electrochemical method has the advantages of low energy consumption, no secondary pollution, small

* Corresponding author.

industrial application area, and simple operation [4,17,18]. Numerous studies have shown that the electrochemical method can effectively remove organic pollutants from aqueous solutions [4,16,19].

The electrode composition is a critical factor that affects electro-catalytic reaction [20]. Foam nickel (Ni) is considered to be one of the most suitable materials for electro-catalytic electrode owing to its easy processing, good stability, and large specific surface area [21–23]. The electrodeposition of palladium (Pd) micro/nanoparticles onto preformed electrodes is a research hotspot. In particular, the dispersion of metal particles improves the electrocatalytic performance of the electrode system [20,24]. Xu et al. [25] reported that Pd–Pt bimetallic nanoparticles have high reduction performance for the catalytic reduction of p-nitrophenol and azo dyes. Wu et al. [26] found that Ni/Pd foam electrode has excellent catalytic performance for para-chloronitrobenzene dechlorination because of the spongy structure of foam Ni and the catalytic activity of Pd. In order to further increase the electro-catalytic activity of the electrode system, many researchers have introduced conductive polymers into the composite electrode because the polymer has a high specific surface area and the stable three-dimensional structure that can increase the dispersion of the catalytic particles [27,28]. Li et al. [20] showed that Pd nanoparticles electrolytic can be uniformly deposited onto electrodes coated with polypyrrole film and the Pd/polypyrrole/foam Ni electrode is effective for the dechlorination of 2,4-dichlorophenol with the removal rate of 90.9%. Polyaniline is cheap, stable in air and easy to get, and electrically conductive polyaniline can be gotten by protonic acid doping [27,29]. In this study, the Pd/PANI/Ni composite electrode was prepared and characterized, and then used to electro-catalyze the degradation of MO in simulated wastewater, the catalytic effect of the substrate electrode on MO being used as a control. At last the stability of the modified electrode was evaluated.

2. Experimental

2.1. Materials

Palladium chloride (99% purity), aniline (99.5% purity), p-toluene sulfonic acid (99.8% purity), and other reagents all were of analytical grade. The foam Ni substrate was purchased from Guangjiayuan Electronic Materials Business Department of Yushan Town in Kunshan City (China) with a size of 30 mm (width) × 40 mm (height) × 1 mm (thickness). The experimental water was ultrapure water with the electricity resistance of 18.3 MΩ × cm and the conductivity of <0.2 μs/cm.

2.2. Electrode preparation

2.2.1. Electrode pretreatment

The graphite plate electrode was immersed in 1.0 mol/L hydrochloric acid overnight, and then washed three times with deionized water after washed three times with acetone. The foam Ni electrode was sonicated in acetone for 15 min and in deionized water for 20 min, and then the cleaned foam Ni electrode was preserved in ultrapure water for further use.

2.2.2. Preparation of modified electrode

The foam Ni electrode pretreated was used as the base material. Polyaniline and Pd were electrodeposited by constant current method in a three-electrode electrochemical workstation. In preparing modified electrode, the foam Ni was used as the working electrode, graphite plate [30 mm (width) × 50 mm (height) × 5 mm (thickness)] was as the counter electrode and the saturated calomel electrode was as the reference electrode. The polymerization conditions were according to the reported procedure [21]. Polyaniline was electrodeposited in 250 mL solution containing 0.1 mol/L aniline and 0.2 mol/L p-toluene sulfonic acid, with the fixed current of 96 mA, the temperature of 0°C and the time of 20 min. The electrode surface of polyaniline was emerald green. Electrodeposition of Pd in 250 mL solution with 1 mmol/L Pd chloride and 3 mmol/L sodium chloride for 2 h was performed under the fixed current of 24 mA and the temperature of 40°C. The electrode surface with Pd turned black and the solution changed from black to colorless.

2.3. Analytical methods

The morphology of Pd/PANI/Ni electrode and Ni foam electrode was determined by using a field emission scanning electron microscopy (JEOLJM-7800F, Japan). Cyclic voltammetry (CV) and alternating current (AC) impedance spectroscopy were measured using a three-electrode electrochemical workstation (CHI660E, Shanghai Chenhua Instrument Co., Ltd.) with a graphite electrode used as a counter electrode, and a saturated calomel electrode as a reference electrode. The data acquisition card (ART DAM3232, Beijing Altai Technology Development Co., Ltd., Beijing, China) was used for recording the real-time change of the external circuit current. The MO concentration was determined by using ultraviolet-visible (UV-vis) spectrophotometer (Beijing Pushi General Instrument Co., Ltd., Beijing, China) at a wavelength of 464 nm. Chemical oxygen demand (COD) was measured according to the standard method of the State Environmental Protection Administration of China.

2.4. Degradation experiment of MO

2.4.1. Experimental device

The rectangular organic glass tank (75 mm × 50 mm × 100 mm) was adopted as the degradation test reactor (as shown in Fig. 1) with an effective volume of approximately 250 mL. The graphite plate electrode, the modified composite electrode (or the foam Ni electrode) and the saturated calomel electrode (CHI150, $E_0 = 0.241$ V vs. NHE at 25°C) were used as the anode, the cathode, and the reference electrode, respectively. The electrolytic solution with 30 mg/L MO and 0.05 mol/L sodium sulfate was used for catalytic degradation at room temperature for 8 h under the voltage of 0.6, 1, 2 V. Decoloration rate is calculated as:

$$R = \frac{A_0 - A_t}{A_0} \times 100\% \quad (1)$$

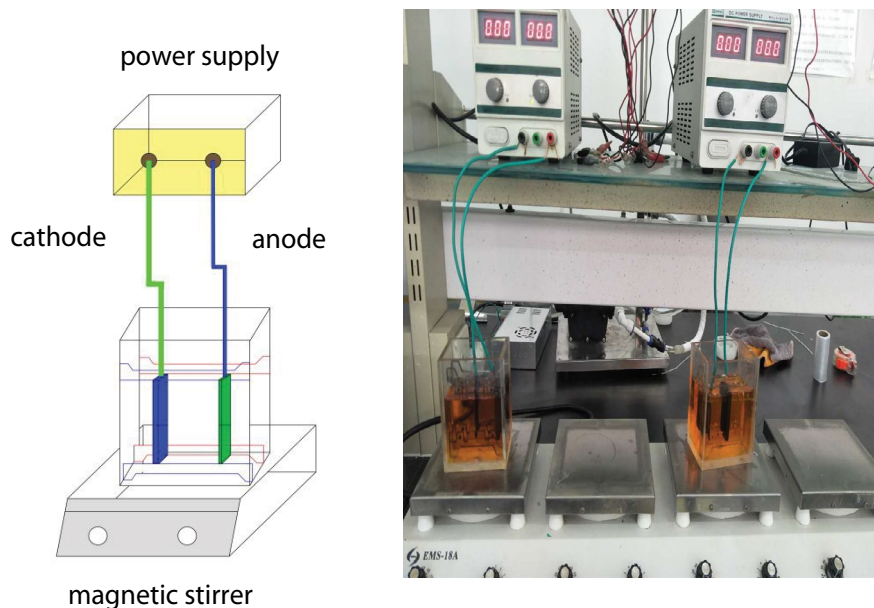


Fig. 1. Experiment device diagram.

where R is the decoloration rate, A_0 is the initial absorbance value, and A_t is the absorbance value at t time.

The degradation rate of MO is calculated as:

$$RE = \frac{C_0 - C_t}{C_0} \times 100\% \quad (2)$$

where RE is the degradation rate, C_0 is the initial MO concentration, and C_t is the MO concentration at t time.

3. Results and discussion

3.1. Electrode characteristics

The morphology of the electrode surface can be analyzed from scanning electron microscope (SEM) images. The SEM images of the pretreated foam Ni electrode, the newly modified electrode, and the used modified electrode were shown in Fig. 2. The surface of the foam Ni electrode was cage-like structure and many small protrusions were seen in 5,000 \times multiple images (Fig. 2a), which was in accord with the previous reports [23,30,31]. The surface of the modified foam Ni changed a lot (Fig. 2b). The predominated growth direction on the foam Ni substrate was perpendicular to the surface of the electrode and the uniform distribution of cluster morphology showed that the growth rate was uniform. Polyaniline has good electrical conductivity, high specific surface area, and good dispersibility for polymeric Pd [31,32]. Polyaniline doped with p-toluene sulfonic acid was applied to the foam Ni electrode for the degradation of pollutants, which greatly increased the specific surface area of the substrate electrode.

In order to investigate the electro-catalytic properties of the modified electrode and the substrate electrode for MO degradation, the CV test was performed under the scanning range of -1.2 – 1.2 V, the scanning speed of 10 mV/s, and the sampling interval of 1 mV. The solution with 30 mg/L MO

and 0.05 M sodium sulfate was used in the two same reactors. There were two pairs of obvious redox peaks in CV curve of the modified electrode (Fig. 3a), the reduction peak potentials being $E_{p1\text{modification}} = -0.507$ V and $E_{p2\text{modification}} = -0.091$ V with the corresponding peak currents of $I_{p1\text{modification}} = 0.1074$ A and $I_{p2\text{modification}} = 0.1044$ A. There was only one pair of redox peaks with weak peak current in the CV curve of the substrate electrode, the reduction peak potential being $E_{p\text{substrate}} = -0.507$ V with the corresponding peak current of $I_{p\text{substrate}} = 0.0024$ A. In the CV test, MO could undergo the fast corresponding reduction reaction at the peak potential. The peak current response of the modified electrode was much larger than that of the substrate electrode, therefore the reaction on the modified electrode was more sensitive to the change of the electrode potential than that of the substrate electrode during the degradation of MO. That indicates the electro-catalytic activity of the modified electrode was higher than that of the substrate electrode.

Electrochemical impedance spectroscopy was used to evaluate the catalytic performance of the modified electrode and the substrate electrode. The AC impedance spectra are composed of a semicircle with a high frequency and a straight line with a low-frequency region. The resistance reflected in the high-frequency region mainly consists of the ionic resistance of the electrolyte, the charge transfer resistance in the electrode process, and the Faraday impedance caused by the diffusion process [30,33,34]. Impedance tests were performed on the modified electrode and the substrate electrode at the test frequency of 10^5 – 10^{-2} Hz and the amplitude of 5 mV. The corresponding equivalent circuit diagram was shown at the upper-right corner in Fig. 3b. R_1 is the ionic resistance in the electrolyte, R_2 represents the electrode surface charge transfer resistance, and R_3 represents the adsorption-related Faraday impedance [35–38]. The experimental data were fitted by Zview software. The solution resistance R_1 in the modified electrode reactor was 3.207 Ω similar to the substrate

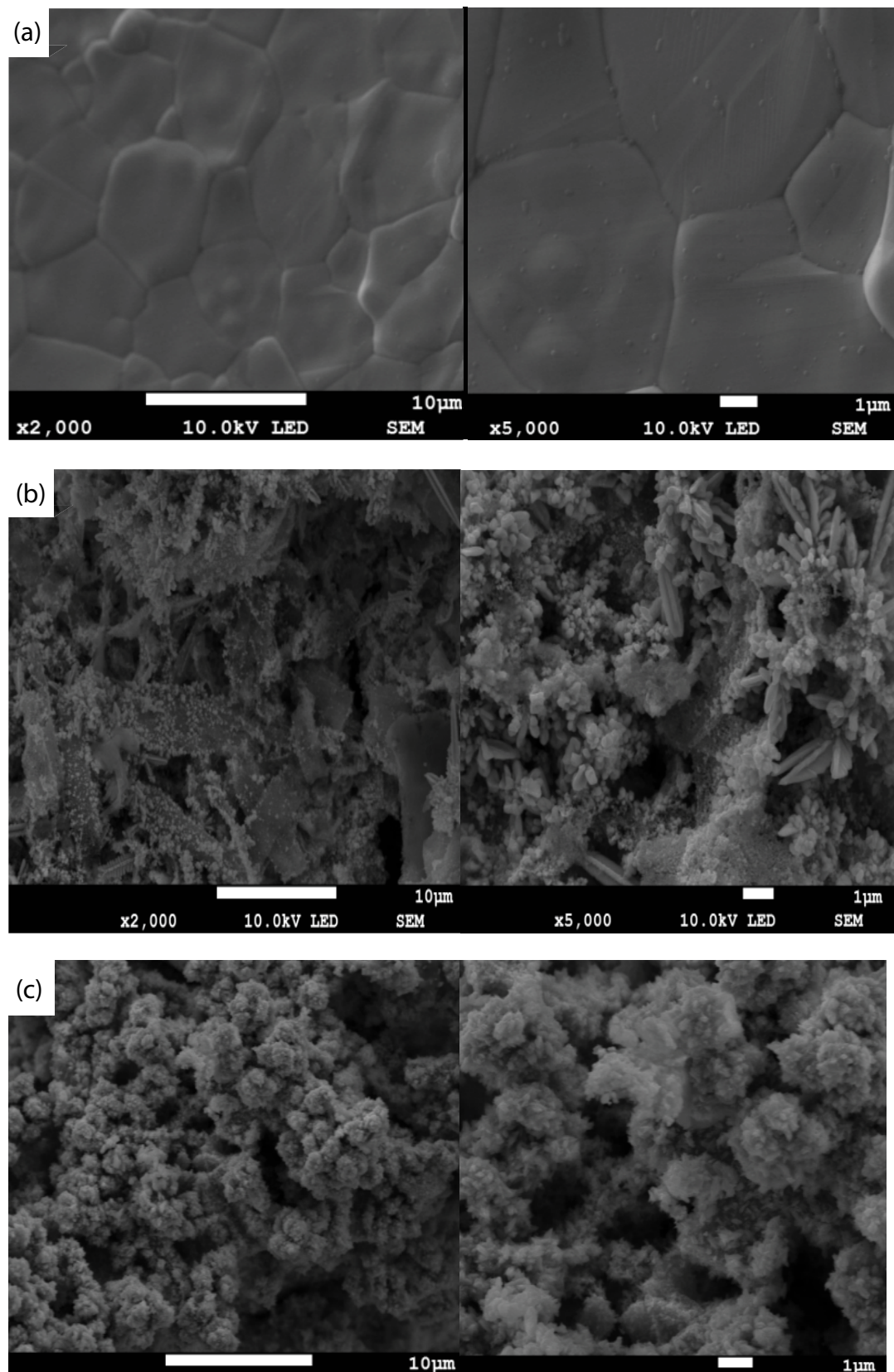


Fig. 2. SEM images of (a) foam nickel electrode, (b) newly prepared Pd/PANI/Ni electrode, and (c) Pd/PANI/Ni electrode used multiple times.

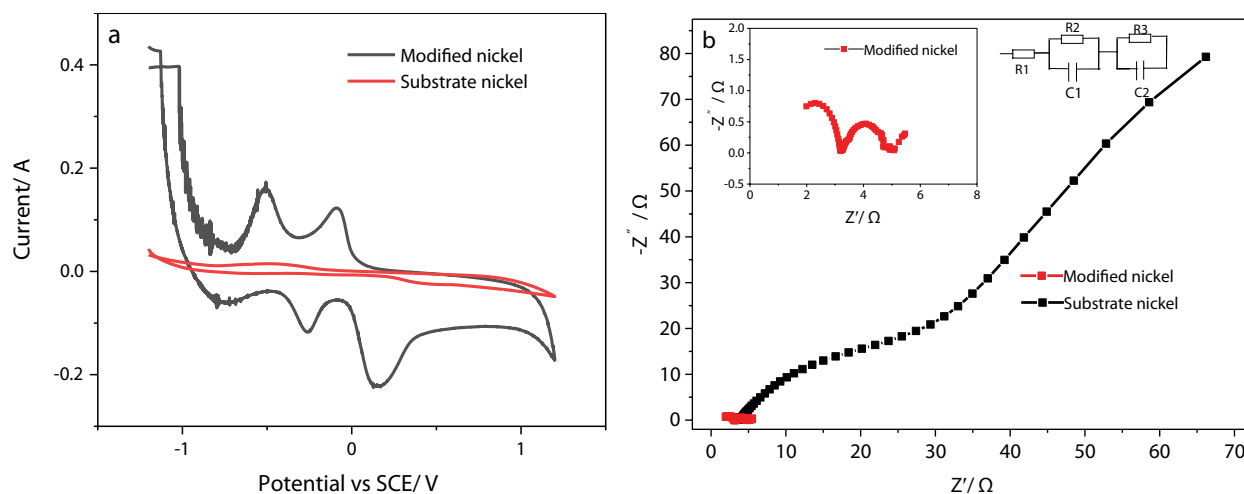


Fig. 3. (a) Cyclic voltammograms of the two electrodes and (b) AC impedance spectra of the two reactors.

electrode reactor (3.257Ω), because of the electroconductive inorganic ions in the electrolyte solution of the reactor was the same. The charge transfer resistance R_2 of the modified electrode (0.539Ω) was far less than the substrate electrode (6.36Ω), indicating the modified electrode had a faster charge transfer rate than the substrate electrode. That probably increases the degradation rate of pollutants. The R_3 value (4.783Ω) of the modified electrode was larger than the substrate electrode (3.526Ω), indicating that the electrode surface was more hydrophilic after modification and the adsorption of pollutants on the modified electrode was lowered.

3.2. MO degradation

3.2.1. Effect of voltage on the removal of MO

The voltages of 0.6, 1, and 2 V were employed to study the removal of MO and the adsorption of MO on the modified electrode (without electricity) was also investigated. The experimental water with 0.05 M sodium sulfate and 30 mg/L MO was the same as that in the CV test (Section 3.1) and the room temperature was 20.5°C. The experimental results were shown in Fig. 4. The MO content decreased from 30 to 28 mg/L in 1 h on the modified electrode without electricity, that is, the adsorption removal was 2 mg/L, indicating that the modified electrode had certain adsorption for MO. MO decreased from 30 to 27.5 mg/L on the foam Ni substrate electrode (Fig. S1a). The adsorption amount of the contaminant onto the substrate electrode was greater than that of the modified electrode, which was related to the hydrophilicity increase of the modified electrode. When the applied voltage was increased from 0.6 to 2 V, the removal efficiency of MO and the decoloration rate increased greatly (Figs. 4a and b; Figs. S1a and b). The MO concentration decreased to 8 mg/L at 1 V and 15 mg/L at 0.6 V and the decoloration rate only reached 75% at 1 V and 50% at 0.6 V in 8 h and the MO concentration dropped to zero and the decoloration rate reached 97% at 2 V in 8 h in the modified electrode reactor. According to the results of the kinetic fitting, the degradations of MO for the substrate electrode and the modified electrode both were

first-order reactions at 2 V. The rate constants were: $k_{\text{substrate}} (0.403 \text{ h}^{-1}) < k_{\text{modified}} (0.472 \text{ h}^{-1})$ with the two-reactor correlation coefficients $R^2 > 0.97$ (Fig. S1d). More significantly, the degradation rate of MO at 2 V was much faster than the other two voltages during the initial 2 h. That is probably related to a faster charge transfer rate under higher electric field intensity.

The trend of the COD removal rate was similar under the three voltages (Fig. 4c). The COD removal rate increased rapidly in the first 2 h, then slowly increased, and finally stabilized. The COD removal rates (52% at 2 V, 39% at 1 V, and 35% at 0.6 V) for the modified electrode were higher than those (38% at 2 V, 31% at 1 V, and 26% at 0.6 V) for the foam Ni electrode (Fig. S1c). The modified electrode was favorable to the degradation of MO and its intermediates.

3.2.2. UV-vis absorption spectrum

Fig. 4d showed the UV-Vis spectra before and after electrochemical treatment of MO. There were two obvious absorption peaks at 270 and 464 nm in the initial solution. The weak absorption peak at 270 nm in the ultraviolet region is related to the benzene ring while the main absorption peak at 464 nm in the visible region is related to azo structure in MO molecules [39]. The degradation of MO in the modified electrode reactor was obviously better than that in the substrate electrode reactor at 4 h. The main absorption peaks in the modified electrode reactor and the substrate electrode reactor both decreased with the reaction time extension, indicating that the azo structure in MO molecules was destroyed. That was consistent with the decoloration. The absorption peak in the modified electrode reactor weakened more than that in the substrate electrode reactor, and the main absorption peak basically disappeared at 4 h. A new weak absorption peak appeared at 248 nm in the two reactors, which may be related to the small molecule compound with benzene ring structure generated after the azo structure in the MO molecule was decomposed. The new compound was presumed to be a refractory organic sulfanilic acid. The absorption peak at 248 nm for the modified electrode was weaker than that for the foam Ni electrode,

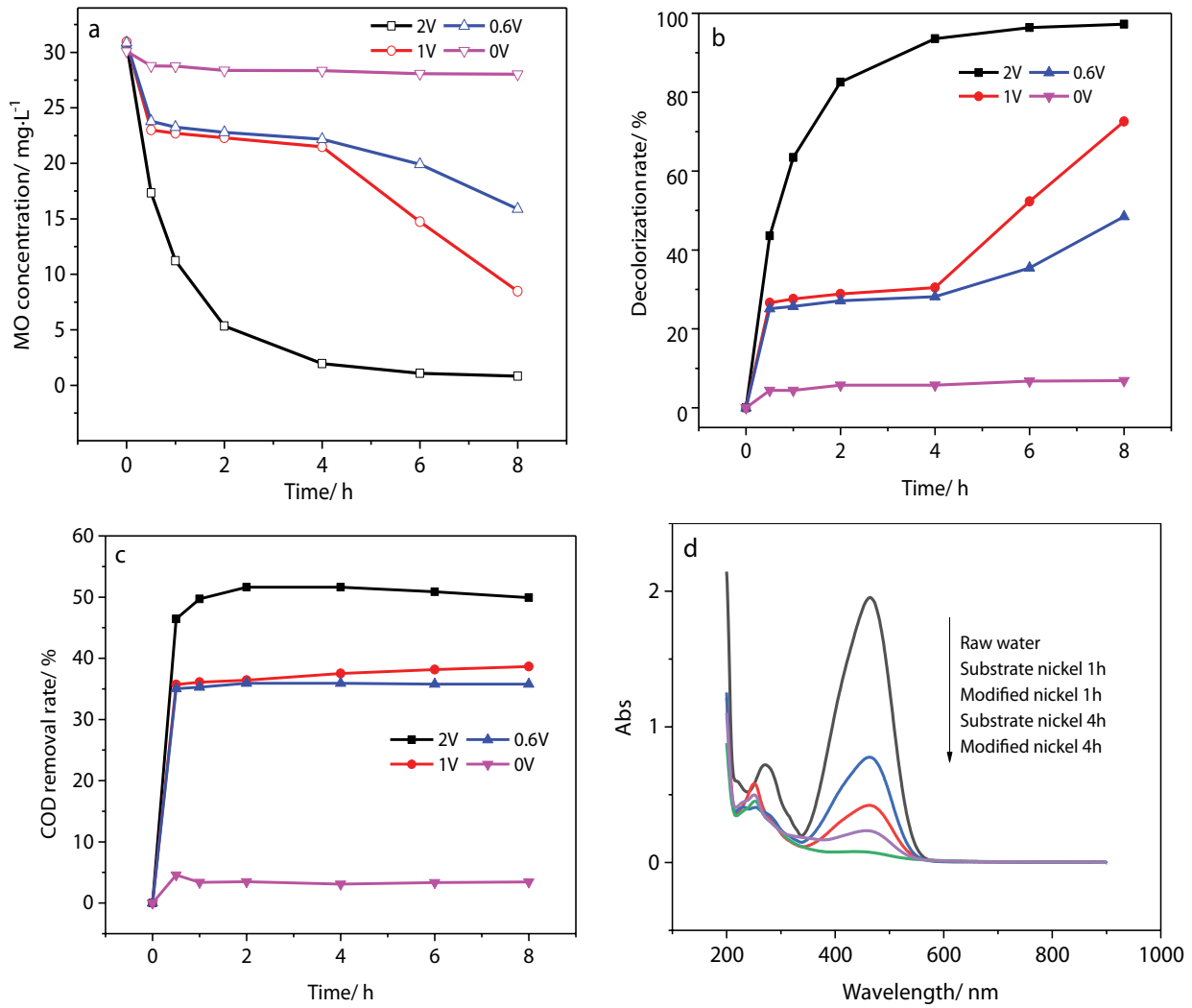


Fig. 4. (a) Concentration of methyl orange, (b) decoloration rate of methyl orange, (c) COD removal rate with time in the modified electrode reactor at 0, 0.6, 1, and 2 V and (d) UV scanning spectra of substrate electrode and the modified electrode at 2 V.

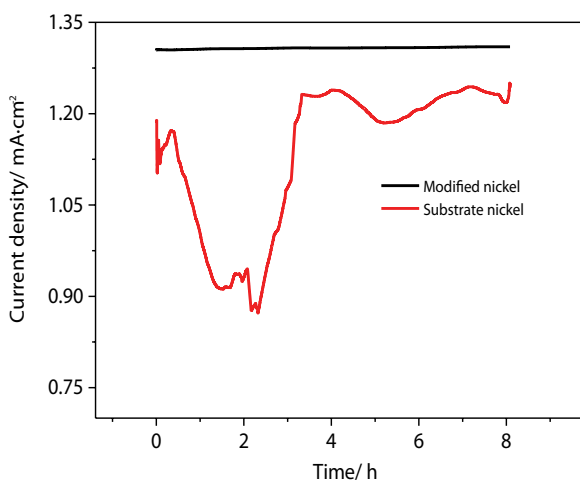


Fig. 5. Variation of the current density of the substrate Ni electrode and the modified Ni electrode overtime in one cycle.

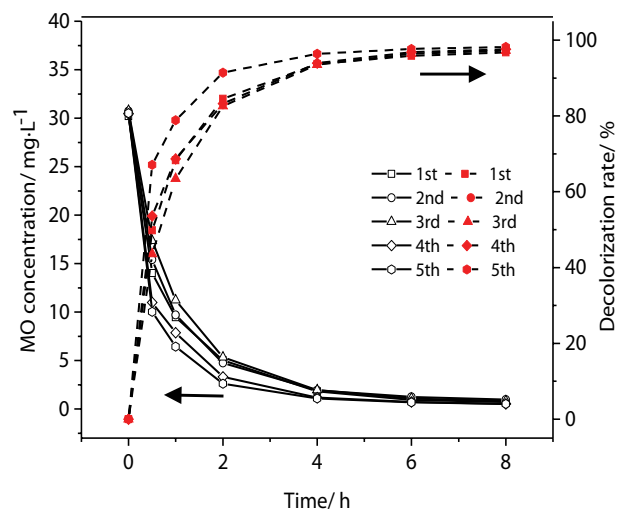


Fig. 6. Recycling of the modified Ni electrode.

revealing the modified electrode was beneficial to the degradation of the intermediates.

3.3. Current density changes in MO degradation

Fig. 5 showed the change of current density overtime in one cycle (8 h) for the MO degradation. The current density of the modified electrode in a cycle was larger than that of the substrate electrode. The result clearly indicated that the chemical reaction in the modified electrode reactor was more intense and the degradation rate of MO was faster. It could be seen from Fig. 5 that the current density of the modified electrode changed little and the current density of the substrate electrode had a wide fluctuation. The current density of the modified electrode was stable, indicating that the modified Ni electrode had excellent MO electro-reduction.

3.4. Reuse of the modified electrode

In order to investigate the stability of the modified electrode, the experiment was carried out five recycles under the voltage of 2 V. After each experiment, the electrode was washed with distilled water to eliminate the error. The experimental result was shown in Fig. 6. With the reaction time extension the MO degradation efficiencies and the decoloration rate could reach ~97% at 8 h for five recycles, showing that its catalytic degradation performance was not weakened obviously. Though Fig. 2c showed that the cluster of modified electrode used was denser than the new electrode, the morphological change affected the catalytic reaction a little. The modified electrode had good stability and could be reused.

4. Conclusions

- The modified Ni electrode was fabricated by two-step electrodeposition and the modified electrode significantly increased its specific surface area, reduced its resistance and enhanced the catalytic activity of MO degradation in comparison with the substrate Ni electrode.
- The degradations of MO by the modified electrode and the substrate electrode at the voltage of 2 V both were first-order reactions and the rate constants were $k_{\text{substrate}}$ (0.402 h^{-1}) < k_{modified} (0.472 h^{-1}). The COD removal rate (52%) for the modified electrode was higher than that (38%) for the foam Ni electrode. The modified Ni electrode was favorable to the degradation of MO and its intermediates.
- Under the voltage of 2 V, the current density of the modified Ni electrode was stable and higher than that of the substrate Ni electrode, indicating that the degradation rate of MO on the modified electrode was faster.
- The modified electrode had good stability and could be reused for MO degradation.

Acknowledgments

This work was supported by the National Natural Science Foundation of China under Grant 51078265; and the

Research Fund of Tianjin Key Laboratory of Aquatic Science and Technology under Grant TJKLAST-PT-13-025.

References

- [1] K. Akansha, D. Chakraborty, S.G. Sachan, Decolorization and degradation of methyl orange by *Bacillus stratosphericus* SCA1007, *Biocatal. Agric. Biotechnol.*, 18 (2019), doi: 10.1016/j.bcab.2019.101044 (In Press).
- [2] N. Bi, H. Zheng, Y. Zhu, W. Jiang, B. Liang, Visible-light-driven photocatalytic degradation of non-azo dyes over Ag_2O and its acceleration by the addition of an azo dye, *J. Environ. Chem. Eng.*, 6 (2018) 3150–3160.
- [3] Z. Kiayi, T.B. Lotfabad, A. Heidarinasab, F. Shahcheraghi, Microbial degradation of azo dye carmoisine in aqueous medium using *Saccharomyces cerevisiae* ATCC 9763, *J. Hazard. Mater.*, 373 (2019) 608–619.
- [4] M.O.A. Pacheco-Alvarez, A. Picos, T. Perez-Segura, J.M. Peralta-Hernandez, Proposal for highly efficient electrochemical discoloration and degradation of azo dyes with parallel arrangement electrodes, *J. Electroanal. Chem.*, 838 (2019) 195–203.
- [5] B. Szadkowski, A. Marzec, J. Rogowski, W. Maniukiewicz, M. Zaborski, Insight into the formation mechanism of azo dye-based hybrid colorant: physico-chemical properties and potential applications, *Dyes Pigm.*, 167 (2019) 236–244.
- [6] B. Merzouk, B. Gourich, A. Sekki, K. Madani, C. Vial, M. Barkaoui, Studies on the decolorization of textile dye wastewater by continuous electrocoagulation process, *Chem. Eng. J.*, 149 (2009) 207–214.
- [7] T.A. Nguyen, R.S. Juang, Treatment of waters and wastewaters containing sulfur dyes: a review, *Chem. Eng. J.*, 219 (2013) 109–117.
- [8] L.L. Zhai, Z.S. Bai, Y. Zhu, B.J. Wang, W.Q. Luo, Fabrication of chitosan microspheres for efficient adsorption of methyl orange, *Chin. J. Chem. Eng.*, 26 (2018) 657–666.
- [9] A.A.A. Darwish, M. Rashad, H.A. AL-Aoh, Methyl orange adsorption comparison on nanoparticles: isotherm, kinetics, and thermodynamic studies, *Dyes Pigm.*, 160 (2019) 563–571.
- [10] M.H. Zhou, H. Sarkka, M. Sillanpaa, A comparative experimental study on methyl orange degradation by electrochemical oxidation on BDD and MMO electrodes, *Sep. Purif. Technol.*, 78 (2011) 290–297.
- [11] V. Deneva, A. Lycka, S. Hristova, A. Crochet, K.M. Fromm, L. Antonov, Tautomerism in azo dyes: border cases of azo and hydrazo tautomers as possible NMR reference compounds, *Dyes Pigm.*, 165 (2019) 157–163.
- [12] L. Fu, Y.N. Bai, Y.Z. Lu, J. Ding, D. Zhou, R.J. Zeng, Degradation of organic pollutants by anaerobic methane-oxidizing microorganisms using methyl orange as example, *J. Hazard. Mater.*, 364 (2019) 264–271.
- [13] Y. Sha, I. Mathew, Q. Cui, M. Clay, F. Gao, X.J. Zhang, Z. Gu, Rapid degradation of azo dye methyl orange using hollow cobalt nanoparticles, *Chemosphere*, 144 (2016) 1530–1535.
- [14] S. Martinez-Lopez, C. Lucas-Abellan, A. Serrano-Martinez, M.T. Mercader-Ros, N. Cuartero, P. Navarro, S. Perez, J.A. Gabaldon, V.M. Gomez-Lopez, Pulsed light for a cleaner dyeing industry: azo dye degradation by an advanced oxidation process driven by pulsed light, *J. Cleaner Prod.*, 217 (2019) 757–766.
- [15] V. Innocenzi, M. Prisciandaro, M. Centofanti, F. Vegliò, Comparison of performances of hydrodynamic cavitation in combined treatments based on hybrid induced advanced Fenton process for degradation of azo-dyes, *J. Environ. Chem. Eng.*, 7 (2019), doi: 10.1016/j.jece.2019.103171 (In Press).
- [16] H.A. Yusuf, Z.M. Redha, S.J. Baldock, P.R. Fielden, N.J. Goddard, An analytical study of the electrochemical degradation of methyl orange using a novel polymer disk electrode, *Microelectron. Eng.*, 149 (2016) 31–36.
- [17] N.P. Shetti, S.J. Malode, R.S. Malladi, S.L. Nargun, S.S. Shukla, T.M. Aminabhavi, Electrochemical detection and degradation of textile dye Congo red at graphene oxide modified electrode, *Microchem. J.*, 146 (2019) 387–392.

- [18] J. Fan, Y. Guo, J. Wang, M. Fan, Rapid decolorization of azo dye methyl orange in aqueous solution by nanoscale zerovalent iron particles, *J. Hazard. Mater.*, 166 (2009) 904–910.
- [19] Z.U. Khan, A. Khan, Y. Chen, A.U. Khan, N.S. Shah, N. Muhammad, B. Murtaza, K. Tahir, F.U. Khan, P.Y. Wan, Photo catalytic applications of gold nanoparticles synthesized by green route and electrochemical degradation of phenolic azo dyes using AuNPs/GC as modified paste electrode, *J. Alloy. Compd.*, 725 (2017) 869–876.
- [20] J. Li, H. Liu, X. Cheng, Q. Chen, Y. Xin, Z. Ma, W. Xu, J. Ma, N. Ren, Preparation and characterization of palladium/polypyrrole/foam nickel electrode for electrocatalytic hydrodechlorination, *Chem. Eng. J.*, 225 (2013) 489–498.
- [21] J.J. Li, C. Luan, Y.Q. Cui, H.X. Zhang, L. Wang, H. Wang, Z.H. Zhang, B. Zhao, H.W. Zhang, X.Y. Zhang, X.W. Cheng, Preparation and characterization of palladium/polyaniline/foamed nickel composite electrode for electrocatalytic dechlorination, *Sep. Purif. Technol.*, 211 (2019) 198–206.
- [22] Y. Liu, L. Liu, J. Shan, J. Zhang, Electrodeposition of palladium and reduced graphene oxide nanocomposites on foam-nickel electrode for electrocatalytic hydrodechlorination of 4-chlorophenol, *J. Hazard. Mater.*, 290 (2015) 1–8.
- [23] Z. Peng, Z. Yu, L. Wang, Y. Hou, Y. Shi, L. Wu, Z. Li, Facile synthesis of Pd–Fe nanoparticles modified Ni foam electrode and its behaviors in electrochemical reduction of tetrabromobisphenol A, *Mater. Lett.*, 166 (2016) 300–303.
- [24] C.H. Nguyen, C.-C. Fu, R.S. Juang, Degradation of methylene blue and methyl orange by palladium-doped TiO₂ photocatalysis for water reuse: efficiency and degradation pathways, *J. Cleaner Prod.*, 202 (2018) 413–427.
- [25] H. Xu, Y. Xiao, M. Xu, H. Cui, L. Tan, N. Feng, X. Liu, G. Qiu, H. Dong, J. Xie, Microbial synthesis of Pd–Pt alloy nanoparticles using *Shewanella oneidensis* MR-1 with enhanced catalytic activity for nitrophenol and azo dyes reduction, *Nanotechnology*, 30 (2019) 065607, doi: 10.1088/1361-6528/aaf2a6.
- [26] Y. Wu, L. Gan, S. Zhang, B. Jiang, H. Song, W. Li, Y. Pan, A. Li, Enhanced electrocatalytic dechlorination of para-chloronitrobenzene based on Ni/Pd foam electrode, *Chem. Eng. J.*, 316 (2017) 146–153.
- [27] Y. Song, J. Song, M. Shang, W. Xu, S. Liu, B. Wang, Q. Lu, Y. Su, Hydrodynamics and mass transfer performance during the chemical oxidative polymerization of aniline in micro-reactors, *Chem. Eng. J.*, 353 (2018) 769–780.
- [28] J.M. Skowroński, J. Urbaniak, Nickel foam/polyaniline-based carbon/palladium composite electrodes for hydrogen storage, *Energy Convers. Manage.*, 49 (2008) 2455–2460.
- [29] L. Shen, X. Huang, Electrochemical polymerization of aniline in a protic ionic liquid with high proton activity, *Synth. Met.*, 245 (2018) 18–23.
- [30] L. Sun, W. He, S. Li, L. Shi, Y. Zhang, J. Liu, The high performance mushroom-like Pd@SnO₂/Ni foam electrode for H₂O₂ reduction in alkaline media, *J. Power Sources*, 395 (2018) 386–394.
- [31] Z. Lou, J. Zhou, M. Sun, J. Xu, K. Yang, D. Lv, Y. Zhao, X. Xu, MnO₂ enhances electrocatalytic hydrodechlorination by Pd/Ni foam electrodes and reduces Pd needs, *Chem. Eng. J.*, 352 (2018) 549–557.
- [32] E. Pargoletti, V. Pifferi, L. Falciola, G. Facchinetti, A. Re Depaolini, E. Davoli, M. Marelli, G. Cappelletti, A detailed investigation of MnO₂ nanorods to be grown onto activated carbon. High efficiency towards aqueous methyl orange adsorption/degradation, *Appl. Surf. Sci.*, 472 (2019) 118–126.
- [33] F.A. Gutierrez, M.D. Rubianes, G.A. Rivas, New bioanalytical platform based on the use of avidin for the successful exfoliation of multi-walled carbon nanotubes and the robust anchoring of biomolecules. Application for hydrogen peroxide biosensing, *Anal. Chim. Acta*, 1065 (2019) 12–20.
- [34] J. Li, W. Qin, A freestanding all-solid-state polymeric membrane Cu²⁺-selective electrode based on three-dimensional graphene sponge, *Anal. Chim. Acta*, 1068 (2019) 11–17.
- [35] H. Zhao, Y. Wu, H. Nan, Y. Du, G. Yang, G. Wang, H. Chen, H. Wei, H. Lin, Preparation and catalytic mechanism of N-TiO₂ based different heterojunction catalytic materials, *Mater. Res. Express*, 6 (2019) 085020.
- [36] N. Ajermoun, A. Farahi, S. Lahrich, M. Bakasse, S. Saqrane, M.A. El Mhammedi, Electrocatalytic activity of the metallic silver electrode for thiamethoxam reduction: application for the detection of a neonicotinoid in tomato and orange samples, *J. Sci. Food Agric.*, 99 (2019) 4407–4413.
- [37] A. Melicchio, E.P. Favvas, Preparation and characterization of graphene oxide as a candidate filler material for the preparation of mixed matrix polyimide membranes, *Surf. Coat. Technol.*, 349 (2018) 1058–1068.
- [38] R.P. Ramasamy, Z. Ren, M.M. Mench, J.M. Regan, Impact of initial biofilm growth on the anode impedance of microbial fuel cells, *Biotechnol. Bioeng.*, 101 (2008) 101–108.
- [39] K. El Hassani, D. Kalnina, M. Turks, B.H. Beakou, A. Anouar, Enhanced degradation of an azo dye by catalytic ozonation over Ni-containing layered double hydroxide nanocatalyst, *Sep. Purif. Technol.*, 210 (2019) 764–774.

Supplementary Information

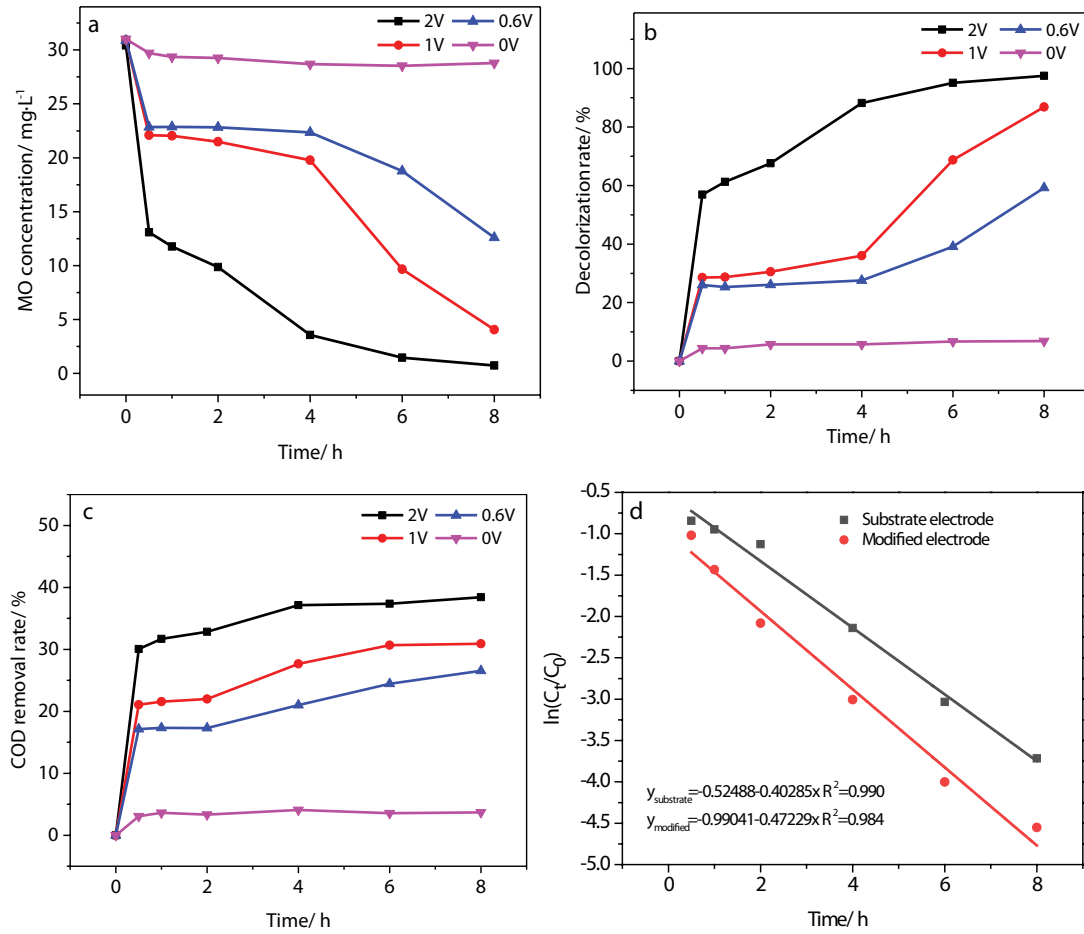


Fig. S1. (a) Concentration of methyl orange, (b) decolorization rate of methyl orange, (c) COD removal rate with time in the substrate electrode reactor at 0, 0.6, 1, and 2 V, and (d) first-order kinetic fitting of the modified electrode and substrate electrode at 2 V.